Clinical Biomechanics 102 (2023) 105891

Contents lists available at ScienceDirect

Clinical Biomechanics

journal homepage: www.elsevier.com/locate/clinbiomech

Reduction of geometric misfit in straight antegrade humeral nailing by evaluating the effect of entry point angulation using a three-dimensional computational analysis

Pivatidevi Pareatumbee [a,1], Suraya Zainul-Abidin [a,b,c], Andy Yew [c,1,*], Tet Sen Howe [a,b,c], Mann Hong Tan [a,b,c], Joyce Suang Bee Koh [a,b,c]

[a] Singhealth-Duke NUS Musculoskeletal Sciences Academic Clinical Program, Singapore General Hospital, Singapore
[b] Department of Orthopaedic Surgery, Singapore General Hospital, Singapore
[c] Division of Musculoskeletal Sciences, Singapore General Hospital, Singapore

ARTICLE INFO

Keywords:
Intramedullary nailing
Entry point
Angulation
Geometric mismatch

ABSTRACT

Background: Straight antegrade intramedullary nails are generally inserted utilising the apex as the surgical entry point in accordance with the mechanical axis of the bone. Our objective is to optimise the bone-nail fit in intramedullary nailing by subjecting the surgical entry point to varying angulations in both the mediolateral and anterior-posterior directions via a quantitative fit assessment in each configuration to identify the optimal angulation, defined as the angulation with the lowest occurrence of thin-out to improve nail fitting within the humerus.

Methods: Computed tomography (CT) scans from 10 cadaveric humeri models were used to generate three-dimensional bone models. The centreline profile of each humerus model was determined by dividing the humerus into multiple slices and identifying its respective centroid. The guidewire and nail models were then established and inserted into the humerus using the apex as the standard entry point. The bone-nail fit was measured utilising three fit quantification parameters: thin-out distance, nail protrusion volume into the cortical shell and deviation distance (top, middle, bottom) between the nail's longitudinal axis and medullary cavity centroid.

Findings: Results revealed a statistically significant association between angulation and occurrence of thin-out ($p < .001$) and showed that the optimally angulated entry point resulted in decreased cortical breach across the nail insertion depth compared to the standard entry point.

Interpretation: Our findings suggested that the current straight nail design may require further modifications to optimise the nail trajectory within the medullary canal by decreasing the bone-nail geometric mismatch to potentially maximise its working length.

1. Introduction

Humeral shaft fractures are a common upper extremity fracture with an occurrence of 1% to 3% in the musculoskeletal trauma patient group and with a reported annual fracture incidence of 14.5 per 100,000, generally in patients over 50 years of age (Court-Brown and Caesar, 2006; Ekholm et al., 2006). There are various cases demanding surgical intervention for humeral shaft fractures such as unstable reduction, open injuries, pathological, segmental and transverse fractures (Walker et al., 2011). From both a biological and biomechanical standpoint, intramedullary (IM) nailing is an attractive option and a standard procedure in today's orthopaedic trauma surgery, conferring better biomechanical stability in comparison to other fixation techniques in the matter of promoting load sharing, allowing shorter union time, full weight-bearing, maintaining periosteal blood supply and also indicated better short-term results in the elderly patient group suffering from serious morbidities (Micic et al., 2019; Ren et al., 2021; Zhao et al., 2015). Furthermore, compared to IM nailing, plating fixation was found

* Corresponding author at: Academic Clinical Program-Musculoskeletal Sciences, Division of Musculoskeletal Sciences, Singapore General Hospital, The Academia, 20 College Road, 169856, Singapore.
E-mail address: andy.yew.k.s@sgh.com.sg (A. Yew).
[1] Both Pivatidevi Pareatumbee and Andy Yew are co-first authors for this manuscript.

https://doi.org/10.1016/j.clinbiomech.2023.105891
Received 27 June 2022; Accepted 10 January 2023
Available online 12 January 2023

to be 2.19 times more susceptible to failure (Hussain et al., 2016). It has proven to be beneficial when treating segmental, highly comminuted, osteoporotic or pathological fractures with an increase in its use noted in recent years (Lopiz et al., 2014). Failure modalities documented in IM nailing and internal fixation include nail migration, implant loosening, screw cut-out and loss of reduction which were highlighted as the most frequent causes of revision surgery (Allende et al., 2014; Dilisio et al., 2016; Krappinger et al., 2011; Lopiz et al., 2014).

One of the challenges encountered in humeral nailing involves navigating an intramedullary device through a narrow humeral canal, especially in smaller profile patients. It is well-known that the selection of the correct nail insertion point is essential for the axial alignment of bone fragments. Iatrogenic fractures can be considered as one of the complications to avoid upon nail insertion (Rommens et al., 2008). According to a study aiming to investigate the humeral canal anatomy when fitting a straight nail into the bone, it was found that the smallest medullary cavity width occurred along the distal third of the humeral shaft. Addtionally, it has also been illustrated that female humeri have a significantly lower cortical thickness compared to male humeri (Schwarz et al., 2020). Understanding the anatomical variation within the humeral canal as well as proper implant fitting is key to prevent such complications (Wozasek and Zak, 2018). Likewise, a study investigating the humeral geometry to find the ideal entry points in antegrade humeral nailing divulged a significant deviation between the cortical bone and intramedullary cavity centre relative to the guidewire centre in certain regions which experienced a substantial posterior bend in relation to the bone's mechanical axis suggesting that the humerus indeed follows a variable curved geometry instead of a straight profile from the superior to the inferior portion of the humerus (Zainul Abidin et al., 2017).

Straight antegrade humeral nailing based on a straight nail design is a newly developed method, utilising a central entry point and serving as a load carrier and has illustrated its mechanical superiority when compared to bent humeral nailing. Additionally, several studies have also highlighted the rate of screw loosening and backout to be approximately 4 to 26% in curved nails in comparison with straight nails (Sharma et al., 2017). Utilising straight nail for proximal humeral fixation has demonstrated a decrease in both the reoperation rate from 42% to 11.5% and rotator-cuff related symptoms when compared to curvilinear nails (Lopiz et al., 2014). Using an insertion point on the rotator cuff is known to be a concern and contributing factor for the increased rate of unsatisfactory outcomes such as persistent pain and is considered as one of the major adverse reported outcomes. Typically, the apex of the humeral head is used as the insertion point and provides the advantage of minimizing the damage imposed on the rotator cuff if the latter has been selected as the insertion point instead (Hao and Huat, 2017; Johnston et al., 2020; Wong et al., 2016). The straight nail has been shown to be more safer option with regards to the risk neurovascular injury potential owing to the more medial entry point (García-Coiradas et al., 2012). Furthermore, recently developed straight nails have also shown to promote faster bone healing and improved functional outcome during mid-term follow up (Mocini et al., 2021).

We believe that a better understanding of the angular deviation between the axis of the medullary cavity and the longitudinal axis of the nail may provide essential knowledge that can be used to minimise cortical breach and risk of over-reaming and therefore demands further research. Few studies have assessed the fit of tibial nail designs using three-dimensional (3D) computational modelling (Amarathunga et al., 2014; Schmutz et al., 2010). A 3D fit assessment may be considered as a superior option in comparison to utilising planar radiographs for conducting a fit assessment in terms of the effectiveness in the prediction of the bone-nail misfit, due to certain limitations such as the inability of a radiograph to reflect the true bone-nail fit with the same level of accuracy and the presence of an unknown amount of distortion and magnification (Schmutz et al., 2010). The objective of this study is to determine whether an optimal nail trajectory can be achieved by imposing minor angulations to the straight nail to improve nail fitting within the curved humeral bone to potentially improve the distal working length within the flat and narrow medullary canal of the humeral shaft. We hypothesize that a nail placed in an optimally angulated trajectory will result in decreased cortical breach.

2. Materials and methods

2.1. Establishment of three-dimensional models of the bone, guidewire and nail

Computed tomography (CT) scans of 10 cadaveric humeri (9 left and 1 right) with a scan resolution of 0.6 mm in all planes in Digital Imaging and Communications in Medicine (DICOM) format were processed in 3D Slicer (Version 4.11) to create 3D solid models of the humerus acquired from 10 subjects (7 males, 56–76 years; 3 females, 65–76 years). Separate cortical and cancellous bone models were generated based on an automatic threshold-based segmentation to differentiate soft tissue and bone using established threshold ranges of 450–3000 Hounsfield units (HU) for the cortical bone and 150–450 HU for the cancellous bone (Zhao et al., 2018). The 3D models were saved in the STL-file format and then imported into FreeCAD (Version 0.19). The bone models were aligned according to the bone's longitudinal mechanical axis and epicondylar axis to create reproducible alignment across all models. A cylindrical rod of diameter 2.5 mm was modelled to simulate the insertion of a guidewire with similar diameter spanning 66% of the humerus length (L) preceding an IM nail surgery. To represent a straight antegrade humeral nail model, a rod consisting of one cylinder with a diameter of 9.5 mm, length of 0.22 L mm and another cylinder with 8.5 mm diameter, length of 0.44 L mm joined at one end was modelled (MultiLoc Humeral Nails Surgical Technique, 2022). A schematic of the 3D guidewire and nail models are illustrated in Fig. 1a. The standard entry point (SEP) was defined as the apex of the humeral head with origin (0,0), located medial to the sulcus and the greater tuberosity and in line with the medullary canal in both anterior-posterior (A-P) and mediolateral (M-L) views as indicated in Fig. 1b.

2.2. Angulation of nail entry point

To investigate the effect of angulation on bone-nail fit, the guidewire was subjected to angulation ranging from 0° to 2° in the M-L and A-P directions considering the angulation between the bone's mechanical axis and the cancellous best fit line, calculated using the centroids across each section along the length of the medullary cavity. A total of 25 combinations, each with a unique angulation in the posterior, anterior, medial and lateral directions were generated as shown in Fig. 1b. A chi-square test for association was then conducted to determine whether there was an association between angulation and the occurrence of thin-out. The optimal angulation, defined as the combination experiencing the lowest occurrence of thin-out across all the models was applied onto the nail model. (See Table 1)

2.3. Quantification of nail fit

Ideally, the best bone-nail anatomical fit can be described as the nail fitting entirely into the medullary cavity of the bone for optimal bone-nail construct stability and preservation of axial alignment. The presence of geometric mismatch between the nail and bone may lead to the protrusion of the nail into the cortical shell. To quantify the degree of geometric mismatch, three parameters were utilised for the quantification assessment of the bone-nail fit in this study as displayed in Fig. 2. Firstly, the thin out distance, was defined as the distance at which the guidewire or nail initially protrudes into the cortical shell along the diaphysis. Secondly, the protrusion volume was defined as the volume of protrusion of the guidewire and nail into the cortical bone and was calculated by computer graphically subtracting the guidewire and nail

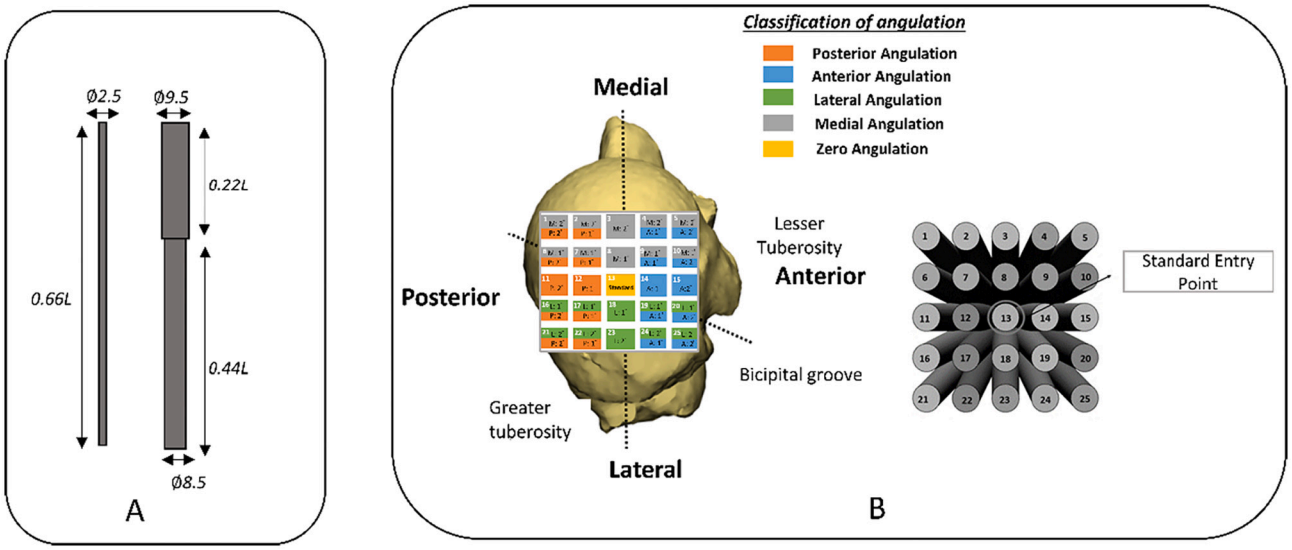

Fig. 1. A) Schematic of guidewire and nail geometry B) Classification of applied angulation combinations (Top humerus view).

Table 1
Crosstabulation of Angulation and Occurrence of thin-out.

	Outcome	
Case	Thin-out	No thin-out
1) $X < 0, Y < 0$	30	10
	(−0.7)	(0.7)
2) $X \geq 0, Y < 0$	58	2
	(3.8)	(−3.8)
3) $X < 0, Y \geq 0$	31	29
	(−6)	(6)
4) $X \geq 0, Y \geq 0$	79	11
	(2.5)	(−2.5)

Note: Adjusted residuals appear in parantheses below observed frequencies.

from the cortical bone. Thirdly, the top, middle and bottom deviation distance defined as the distance between the centroids of the intramedullary canal and the longitudinal axis of the guidewire and nail were measured in the axial plane in both M-L and A-P directions. The results were normalized (Eqs. (1) and (2)) according to the ratio of the distance from the centre of the guidewire or nail to the cortex to the distance from the bone centroid to the cortex at the nail tip. Statistical analysis was conducted on the fit quantification parameters generated by the apex, SEP and the optimal angulated entry point (AEP) using a paired two-tailed Student *t*-test.

The equations can be written as:

$$\%Thin-OutDistance = \frac{Thin-Out\ Distance}{Humeral\ Length} \text{ x } 100\% \quad (1)$$

$$\%ProtrusionVolume = \frac{Cortical \cap Volume}{Volume\ of\ Guidewire/Nail} \text{ x } 100\% \quad (2)$$

2.4. Statistical analyses

All statistical analyses were performed using R (Version 4.2) with a significance level of 0.05.

3. Results

3.1. Evaluating effect of angulation on occurrence of thin-out

A chi-square test for association between angulation and occurrence of thin-out revealed a statistically significant association between angulation and occurrence of thin-out ($p < .001$). The association was relatively strong, Cramer's V = 0.416. Only one combination with an angulation of −1° in the single M-L direction, point 12 generating a 1° posterior angulation as shown in Fig. 1 achieved zero thin-out across all the humeri models and was thus considered to be the optimal angulation.

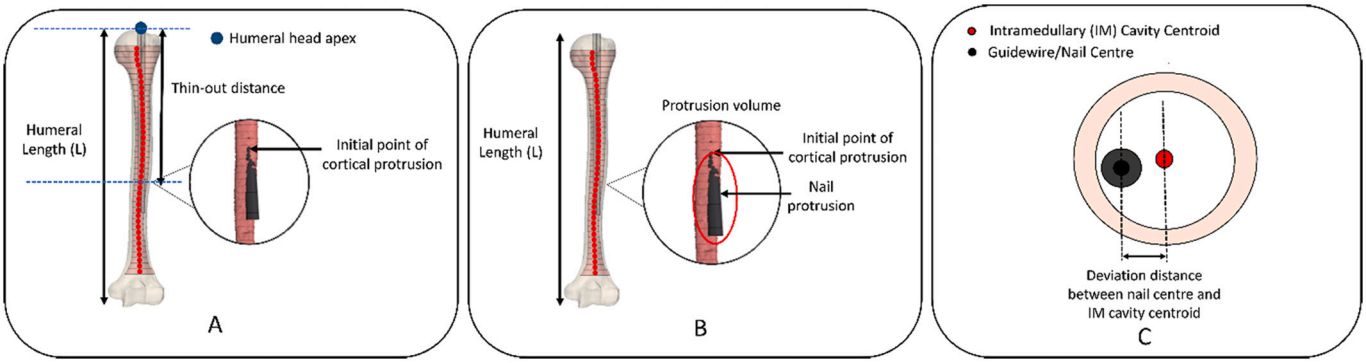

Fig. 2. Measurement of fit quantification parameters. A) Thin-out distance represents the distance between the humeral head apex and the initial point of protrusion of the guidewire/nail into the cortical shell. B) Protrusion volume represents the guidewire/nail volume protruding into the cortical shell. C) Deviation distance represents the distance measured between the intramedullary canal centre and nail centre across an axial plane along the nail insertion depth.

3.2. Comparing fit quantification results between SEP and AEP

3.2.1. Thin-out distance and protrusion

The fit for each individual bone-nail pair was assessed for the SEP and AEP. Statistically significant differences in the protrusion volume ($p = .016$) were observed between SEP and AEP. The presence of protrusion in the virtual bone indicated regions where the bone and nail were forced to deflect which may ultimately lead to improper alignment of main fragments and malreduction depending on the fracture location. The initiation of thin-out was predicted to occur at 67.2% and 52% of the humeral length for for SEP and AEP respectively. The lower magnitude of the %thin-out distance suggested that cortical protrusion occurred more proximally. A fall in the percentage of cortical bone breach from 7.1% to 1% was noticed upon angulation showing that AEP was the optimal entry point in terms % Protrusion Volume with a superior intramedullary nail fit. Additionally, when comparing the total volume of nail protruding from the medullary cavity in the 10 models for the SEP (median: 689 mm^3; range: 1.6 to 2190 mm^3) and AEP (median: 98.3 mm^3; range: 0 to 190 mm^3), it can be deduced that the SEP was approximately seven times more susceptible to cortical protrusion. The total volume of protrusion into the cortical shell and protrusion patterns across the nail insertion depth for the SEP and AEP have been displayed in Fig. 3. The proximal half of the nail inserted using SEP displayed a better intramedullary fit in comparison to when using AEP as the insertion point. A noticeable difference was observed in the degree of protrusion especially from 50% to 100% of the nail insertion depth between SEP, exhibiting a gradually increasing level of protrusion from 0% to 1.1% and AEP, indicating protrusions fluctuating within the range of 0.1% and 0.2%. Overall, the nail with an AEP displayed a better anatomical fit into the intramedullary cavity, representing the space available for nail positioning experiencing a lower mean protrusion volume and smaller protrusion volume across the nail insertion depth.

3.2.2. Deviation distance

Based on the results obtained, a statistically significant difference was only observed in the A-P direction for the top ($p = .001$), middle ($p < .001$) and bottom ($p = .006$) sections. However, no statistically significant differences were obtained in M-L direction for the top ($p = .419$), middle ($p = .277$) and bottom ($p = .357$). The mean and standard deviation for the deviation distance in the axial plane in the M-L direction for the SEP was 1.6 ± 0.4 (top), 2.2 ± 0.1 (middle) and 1.4 ± 0.2 (bottom) and for the AEP, it was 1.6 ± 0.4 (top), 2.2 ± 0.1 (middle) and 1.3 ± 0.2 (bottom). In the A-P direction, the mean and standard deviation for the SEP was 1.4 ± 0.4 (top), 1.3 ± 0.2 (middle) and 3.3 ± 1.2 (bottom) and for the AEP, it was 2.1 ± 0.8 (top), 2.0 ± 0.1 (middle) and 1.9 ± 0.1 (bottom) as illustrated by Fig. 4. Only minimal differences in the deviation distance were found between the SEP and AEP in the M-L direction, in contrast to the A-P direction, which exhibited larger differences in the deviation distance across all sections with the bottom deviation being the most prominent.

4. Discussion

This study presented a useful technique for investigating the influence of angulation on the bone-nail fit, making use of engineering tools such as image processing and reverse engineering to generate a 3D bone model and study the same entry point under multiple angular configurations using 3D modelling software. Like any other procedure, it is vital to optimise fracture treatment by ensuring proper bone-nail fit and nail positioning in the medullary canal. The nail entry point also plays an important role in terms of axially aligning the main bone fragments and preventing iatrogenic fractures upon nail insertion.

It is essential to validate computational models in order to ensure a good quality model with a suitable level of accuracy to address research questions with the maximum level of certainty according to Viceconti et al. (Viceconti et al., 2005; Viceconti et al., 2021). Hence, a convergence analysis based on the STL triangle size by means of reducing the total number of triangles at 25% increments was performed. The convergence results at 0% and 75% resulted in a total protrusion volume of 125 mm^3 and 126 mm^3 respectively as well as %protrusion volume of 1.16 and 1.17 respectively with little to no difference observed within the range of 0.001% to 0.01% in the %thin-out distance and deviation distance. Based on the results, we can conclude that a reduction in the number of triangles did not result in a significant change in the fit quantification parameters. Hence, it is unlikely that the smaller triangles are able to predict different results. With follow-up examinations typically conducted via radiographic assessment such as measuring the bone to implant contact length and implant protrusion length and studies indicating the superiority of CT scans relative to X-ray images for the visualization of fracture extension into the joint space and surgical planning, we assessed the accuracy of our 3D reconstructed model by measuring the diameters of the cortical and cancellous bone in the A-P and M-L direction at every 10% of the humeral length in the CT images with respect to the boundaries of the cortical and cancellous bone and compared with the 3D reconstructed model to ensure optimum accuracy (Avci and Kozaci, 2019; Yu et al., 2021). Results show a percentage

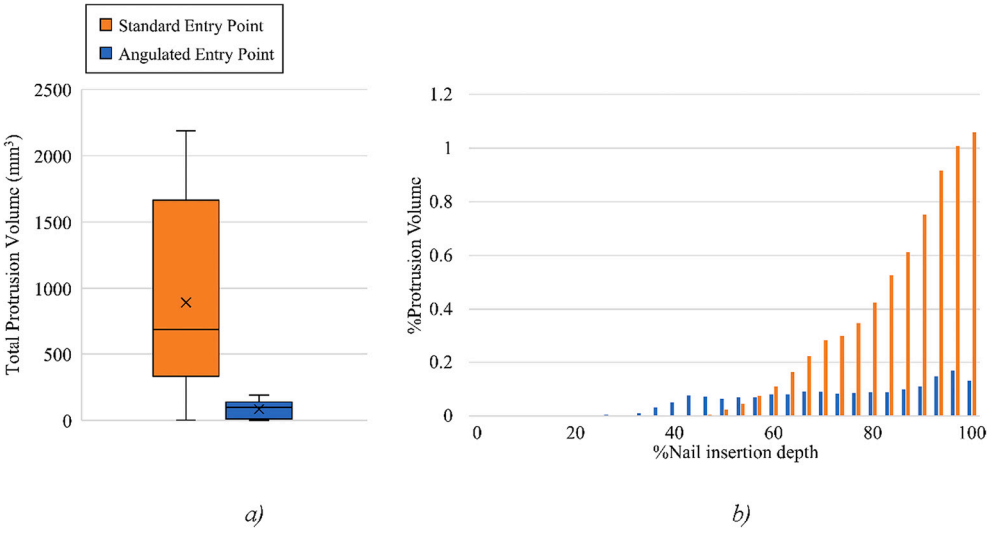

Fig. 3. a) Total protrusion volume for the standard entry point (SEP) and angulated entry point (AEP) b) Protrusion patterns across the nail insertion depth for the standard entry point (SEP) and angulated entry point (AEP).

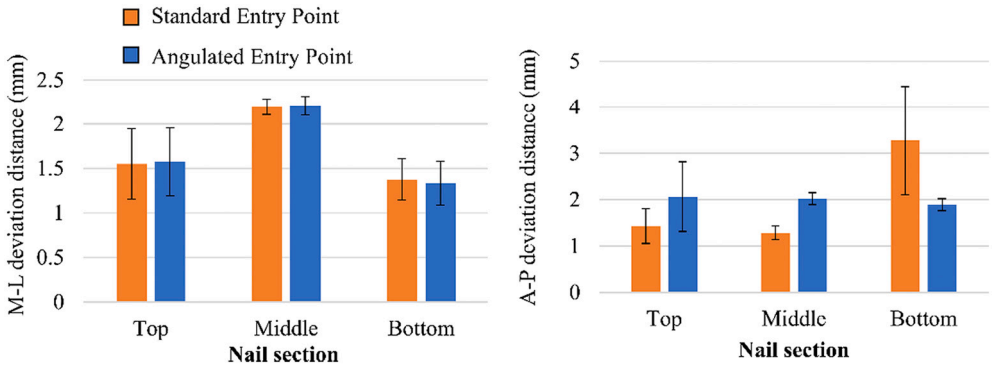

Fig. 4. Deviation distance of SEP and AEP in M-L and A-P direction.

difference within the range of 0.1% to 1.5% between the CT images and the reconstructed model which can be considered to be negligible and as an acceptable level of accuracy to predict the fit quantification parameters in the study, thus, showing that our model is valid.

According to the diagram illustrated in Fig. 5 showing the extent of bone-nail overlap across varying humeral slices, the nail appeared to be centralized within the medullary canal in the proximal humerus, which possessed a larger canal diameter. The likelihood of cortical breach occurring in the top was lower as a consequence of the central placement of the nail within the cancellous bone and its wider cross-sectional area in the proximal portion. The nail inserted according to the SEP experienced a more anterior placement contrary to the AEP, which appeared to be located rather centrally in the mid nail region. Both nails indicated a progressive lateral and anterior deviation starting from the mid-nail to the distal nail end with the SEP displaying a more pronounced deviation and nail protrusion. Based on the results, two varying protrusion patterns were observed. The utilization of SEP lead to a superior fit in the proximal humerus from 0% to 50% of the nail insertion depth with the initiation of thin-out only seen in the mid-nail region in comparison with the AEP which experienced minimal volumes of protrusion more proximally. The AEP maintained a relatively constant degree of protrusion from 50% to 100% of the nail insertion depth, from the mid-nail to the nail tip with only a two-fold increase from 0.06% to 0.13% recorded whereas, the SEP experienced a continuously rising level of protrusion increasing from 0.02% to 1.06% as depicted in Fig. 3. Besides, the nail with an AEP experienced an overall smaller protrusion volume which can be evidently supported by the lower anterior deviation in the bottom section. Hence, it was concluded that the AEP displayed a superior intramedullary fit with reduced cortical breach. Taking into account the decreased canal diameter in the bottom section across the nail insertion depth, it was apparent that the bottom section was susceptible to higher levels of protrusion. Statistically significant differences were solely noted in the A-P deviation distance signifying that it may possibly be a pivotal contributor to cortical breach. The following parameter may indeed serve as a potential design consideration when selecting the implant shape.

To attain optimal alignment in the intramedullary canal, slight adjustments posteriorly about the M-L axis can be made to overcome the geometric mismatch. Nonetheless, angulating the nail with such accuracy remains a challenging task with the lack of surgical instruments capable of generating such precision during a surgical procedure. Currently commercially available antegrade humeral nail designs are not patient-specific or tailored to the morphology of fracture with certain nails consisting of in-built bends ranging from 4 to 6 degrees (Intramedullary nail system for humeral shaft and proximal humeral fractures, 2021; T2 Humeral Nailing System, 2021). Whilst this may be corrected via an acceptable angular malreduction in fractured humeral shafts, an insufficient distal bend could theoretically result in distal peri-implant fractures in prophylactic nailing of narrow humeral canals. The inclusion of an in-built posterior angulation of 1° into the current straight nail design, with the % thin-out distance serving as a reference point for the creation of a minor angulated distal bend may be a possible design consideration for future development of IM nails.

In simulated nail fits for intact bones, this has relevance in prophylactic nailing for impending pathological fractures of the humerus. The distal fit could impact the likelihood of sustaining a peri-implant fracture in the distal humerual shaft. In addition, entry point angulation may impact the nailing of proximal humeral fractures, an indication increasingly common for recent nail designs. It is well recognised these fractures are deformed by the surrounding muscular forces, and must be preliminarily reduced to identify an appropriate entry point. Minimizing entry point angulation will likely reduce subsequent malreduction of

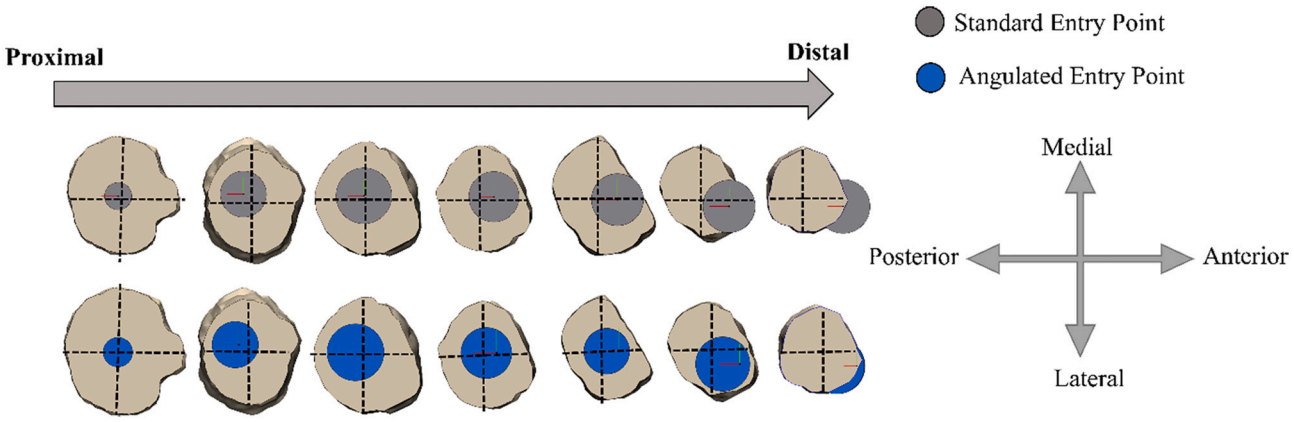

Fig. 5. Cross-sectional view of nail placement across multiple humeral slices from the proximal to the distal end when using SEP and AEP as the nail insertion point.

these fractures which may in turn result in malunion or even non-union.

There are a few advantages of using the following computational technique. The proposed method is not only non-invasive but also able to study the effect of numerous parameters with a high level of precision. This technique can be further developed into an automated or semi-automated process to identify the nail placement with minimum geometric bone-nail mismatch instead of performing physical experiments using multiple cadaver specimens which can be more costly. Utilising cadaveric bones for the evaluation of the effect of angulation on the nail insertion point will be a challenging task especially with such a narrow range and also because the current surgical instruments lack the ability to generate such precise angulations.

There are a few shortcomings in this study. Firstly, the nail diameter was considered to be constant across all the humeri models to better understand the effect of angulating the entry point as opposed to reality, where the nail diameter is generally dependent on the patient's anatomical profile. Secondly, the employment of an approximate geometric representation of the straight nail through the unification of two cylinders of two different diameters may result in minor geometrical differences from the original nail design. Thirdly, only ten humeri cadavers were utilised in this study, which is not sufficient to account for the entire population with a greater range of anatomical profiles. The effect of reaming which is usually performed prior to implantation was also not included in this study and its effect has yet to be understood. The possibility of noise may also affect the measurement accuracy and its effect is also unknown. Furthermore, in virtue of the differences in implant types and anatomical site and scarcity in literature pertaining to 3D computational analyses of the humerus, no direct comparison can be made with prior data. Lastly, our modelling approach was not validated owing to the complexity and cost involved in performing a physical validation.

To our knowledge, this is the first study presenting a method using 3D computational analysis as an attempt to understand the effect of nail positioning of straight antegrade humeral nails in response to varying angulations by means of a quantitative assessment of the bone-nail fit. The proposed study has potential clinical application especially in pre-operative planning and may also eventually aid implant designers in the development of a new nail design in accordance with the variable geometry of the humerus. By optimizing the nail placement and improving anchorage with the surrounding bone, the rehabilitation process can potentially be shortened in the long run by increasing the stability of the bone-implant system. The expected clinical implication of applying the proposed method may help reduce the geometric misfit, dependent on the bone's geometry and nail design by optimizing the nail trajectory within the medullary canal to avoid angulation deviations in straight antegrade nails as far as possible. Specifically, particular attention need to be paid where wall thin out is already apparent close to the entry point, or in oblique fracture configurations where such deviations may lead to "escape" of the guidewire or reamer with neurovascular injury. This study also emphasizes the potential benefit of prior fracture reduction (close or mini open) not only in optimizing the nail entry point, but also in determining the correct trajectory for the nail. The following method may also serve as a teaching tool for surgeons to visualize the effect of angulation in straight antegrade IM nailing and as a design strategy for engineers to create patient-specific implants or making future improvements of the current nail design.

5. Conclusion

A useful computational modelling technique to study the influence of angulation on the bone nail fit was developed. The presented study revealed that the application of a posterior angulation of 1° with respect to the M-L axis, using the apex as the reference point may result in an optimized bone-nail fit by minimizing the anterior deviation. This optimal nail positioning can be achieved surgically by identifying the M-L axis and apex of the humeral head and ensuring that the top nail centre is collinear with the apex followed by applying a slight tilt to the nail perpendicular to the M-L axis to generate the required posterior angulation, which will in turn allow the nail to achieve a more posterior placement throughout the nail insertion depth. However, this is not achievable by the surgeon in current practice. The obtained results will be useful for implant manufacturers to develop instruments that can help the surgeon with precision positioning and possibly developing nails with smaller and appropriate angulations. Nevertheless, additional studies are needed to validate the potentiality of the above-mentioned approach before extrapolating it to a clinical setting. Future work may also include performing a physical validation of the modelling approach as well as assessing the differences in mechanical stresses and strains upon the utilization of an SEP and AEP to determine the extent of influence of supporting bone around the nail on implant stability.

Acknowledgments

This research was supported by funds from the SingHealth Research Grant (Grant reference number: SHF/FG629S/2014).

References

Allende, C., Paz, A., Altube, G., Boccolini, H., Malvarez, A., Allende, B., 2014. Revision with plates of humeral nonunions secondary to failed intramedullary nailing. Int. Orthop. 38 (4), 899–903.

Amarathunga, J., Schuetz, M., Yarlagadda, P., Schmutz, B., 2014. Automated fit quantification of tibial nail designs during the insertion using computer three-dimensional modelling. Proc. Inst. Mech. Eng. H J. Eng. Med. 228 (12), 1227–1234.

Avci, M., Kozaci, N., 2019. Comparison of X-ray imaging and computed tomography scan in the evaluation of knee trauma. Medicina (Kaunas, Lithuania) 55 (10), 623. https://doi.org/10.3390/medicina55100623.

Court-Brown, C.M., Caesar, B., 2006. Epidemiology of adult fractures: a review. Injury 37 (8), 691–697.

Dilisio, M.F., Nowinski, R.J., Hatzidakis, A.M., Fehringer, E.V., 2016. Intramedullary nailing of the proximal humerus: evolution, technique, and results. J. Shoulder Elb. Surg. 25 (5), e130–e138.

Ekholm, R., Adami, J., Tidermark, J., Hansson, K., Törnkvist, H., Ponzer, S., 2006. Fractures of the shaft of the humerus. An epidemiological study of 401 fractures. J. Bone Joint Surg. 88 (11), 1469–1473.

García-Coiradas, J., Rodríguez-Niedenführ, M., López, Y., García-Fernandez, C., Sañudo, J., Vázquez, T., Marco, F., 2012. A new straight proximal humeral nail: a cadaveric study of its anatomical relationships. Eur. J. Anat. 16 (3), 184–189.

Hao, T.D., Huat, A., 2017. Surgical technique and early outcomes of intramedullary nailing of displaced proximal humeral fractures in an Asian population using a contemporary straight nail design. J. Orthop. Surg. (Hong Kong) 25 (2), 2309499017713934.

Hussain, N., Sermer, C., Prusick, P.J., Banfield, L., Atrey, A., Bhandari, M., 2016. Intramedullary nailing versus plate fixation for the treatment displaced midshaft clavicular fractures: a systematic review and meta-analysis. Sci. Rep. 6, 34912. https://doi.org/10.1038/srep34912.

Intramedullary nail system for humeral shaft and proximal humeral fractures, 2021. Retrieved 22 July 2021, from. https://www.jusimed.com.br/site/attachments/article/5/Targon%20PH%20e%20H.pdf.

Johnston, P., Hatzidakis, A., Tagouri, Y., Curran-Everett, D., Sears, B., 2020. Anatomic evaluation of radiographic landmarks for accurate straight antegrade intramedullary nail placement in the humerus. JSES Int. 4 (4), 745–752. https://doi.org/10.1016/j.jseint.2020.06.004.

Krappinger, D., Bizzotto, N., Riedmann, S., Kammerlander, C., Hengg, C., Kralinger, F.S., 2011. Predicting failure after surgical fixation of proximal humerus fractures. Injury 42 (11), 1283–1288.

Lopiz, Y., Garcia-Coiradas, J., Garcia-Fernandez, C., Marco, F., 2014. Proximal humerus nailing: a randomized clinical trial between curvilinear and straight nails. J. Shoulder Elb. Surg. 23 (3), 369–376.

Micic, I., Kholinne, E., Kwak, J.M., Sun, Y., Nanda, A., Kim, H., Koh, K.H., Jeon, I.H., 2019. Humeral diaphyseal fracture nonunion: an audit of the outcome from intramedullary nailing and DCP plating. Biomed. Res. Int. 2019, 9107898. https://doi.org/10.1155/2019/9107898.

Mocini, F., Rovere, G., De Mauro, D., De Sanctis, E.G., Smakaj, A., Maccauro, G., Liuzza, F., 2021. Newer generation straight humeral nails allow faster bone healing and better functional outcome at mid-term. J. Orthop. Surg. Res. 16 (1) https://doi.org/10.1186/s13018-021-02776-w.

MultiLoc Humeral Nails Surgical Technique, 2022. DePuy Sythes. Retrieved October 31.

Ren, C., Li, M., Sun, L., Li, Z., Xu, Y., Lu, Y., Wang, Q., Ma, T., Xue, H., Zhang, K., 2021. Comparison of intramedullary nailing fixation and percutaneous locked plating fixation for the treatment of proximal tibial fractures: a meta-analysis. J. Orthop. Surg. (Hong Kong) 29 (2). https://doi.org/10.1177/23094990211024395, 23094990211024395.

Rommens, P.M., Kuechle, R., Bord, T., Lewens, T., Engelmann, R., Blum, J., 2008. Humeral nailing revisited. Injury 39 (12), 1319–1328. https://doi.org/10.1016/j.injury.2008.01.014.

Schmutz, B., Rathnayaka, K., Wullschleger, M.E., Meek, J., Schuetz, M.A., 2010. Quantitative fit assessment of tibial nail designs using 3D computer modelling. Injury 41 (2), 216–219.

Schwarz, G.M., Zak, L., Hirtler, L., Wozasek, G.E., 2020. Anatomical considerations of intramedullary humeral nailing and lengthening. J. Clin. Med. 9 (3), 806. https://doi.org/10.3390/jcm9030806.

Sharma, G.M., Naik, L.G., Chaitanya, W., Chavan, S., Roy, K., Pawar, P., Tadepalli, K., 2017. Treatment of three-and four-part proximal humerus fractures by MultiLoc nailing technique- a prospective study11. J. Clin. Diagn. Res. 11 (11), 9–11. https://doi.org/10.7860/jcdr/2017/30973.10875.

T2 Humeral Nailing System, 2021. Retrieved 22 July 2021, from. https://www.strykermeded.com/media/1668/t2-humerus.pdf.

Viceconti, M., Olsen, S., Nolte, L.P., Burton, K., 2005. Extracting clinically relevant data from finite element simulations. Clin. Biomech. (Bristol, Avon) 20 (5), 451–454. https://doi.org/10.1016/j.clinbiomech.2005.01.010.

Viceconti, M., Pappalardo, F., Rodriguez, B., Horner, M., Bischoff, J., Musuamba Tshinanu, F., 2021. In silico trials: verification, validation and uncertainty quantification of predictive models used in the regulatory evaluation of biomedical products. Methods (San Diego, Calif.) 185, 120–127. https://doi.org/10.1016/j.ymeth.2020.01.011.

Walker, M., Palumbo, B., Badman, B., Brooks, J., Van Gelderen, J., Mighell, M., 2011. Humeral shaft fractures: a review. J. Shoulder Elb. Surg. 20 (5), 833–844.

Wong, J., Newman, J.M., Gruson, K.I., 2016. Outcomes of intramedullary nailing for acute proximal humerus fractures: a systematic review. J. Orthop. Traumatol. 17 (2), 113–122.

Wozasek, G.E., Zak, L., 2018. Intramedulläre Oberarmverlängerung [Intramedullary upper arm lengthening]. Unfallchirurg 121 (11), 868–873. https://doi.org/10.1007/s00113-018-0542-3.

Yu, Y., Jiang, Q., Zhang, Z., Yu, X., Deng, F., 2021. Influence of implant protrusion length on non-grafting osteotome sinus floor elevation with simultaneous implant: a 3- to 9-year retrospective study. Int. J. Implant Dent. 7 (1), 22. https://doi.org/10.1186/s40729-021-00304-3.

Zainul Abidin, S., Choh, A., Yew, A., Koh, J., Mann Hong, T., 2017. Ideal Entry Points for an Antegrade Humeral Nail: A Three-Dimensional Computational Analysis. Orthopaedic Research Society 2017 Annual Meeting.

Zhao, J.G., Wang, J., Wang, C., Kan, S.L., 2015. Intramedullary nail versus plate fixation for humeral shaft fractures: a systematic review of overlapping meta-analyses. Medicine 94 (11), e599. https://doi.org/10.1097/MD.0000000000000599.

Zhao, L., Tian, D., Wei, Y., Zhang, J., Di, Z., He, Z., Hu, Y., 2018. Biomechanical analysis of a novel intercalary prosthesis for humeral diaphyseal segmental defect reconstruction. Orthop. Surg. 10 (1), 23–31.